

Nb-doped TiO₂ thin films for photovoltaic applications

T. Potlog^{a,*}, P. Dumitriu^a, M. Dobromir^b, A. Manole^b, D. Luca^b

^a Department of Physics and Engineering, Moldova State University, A. Mateevici str. 60, MD 2009 Chisinau, Republic of Moldova

^b Faculty of Physics, Alexandru Ioan Cuza University, 11 Carol I Blvd., 700506 Iasi, Romania

ARTICLE INFO

Article history:

Received 19 January 2015

Received in revised form 1 July 2015

Accepted 6 July 2015

Available online 11 July 2015

Keywords:

Nb-doped TiO₂ thin films

CdTe

Photovoltaic device

ABSTRACT

Polycrystalline titania and Nb:TiO₂ thin films were deposited by RF magnetron sputtering. The influence of post-deposition annealing in vacuum and hydrogen atmosphere on the structure, morphology, oxidation states and optical properties was studied by X-ray diffraction, atomic force microscopy, XPS and UV–VIS spectroscopy. The heat treatment of titanium dioxide thin films in vacuum and H₂ atmosphere induces structural and morphological changes. The band gap narrowing was observed for the transparent as-deposited Nb:TiO₂ films, while annealing at 420 °C in H₂ atmosphere resulted in an enhancement of the electrical conductivity. Further on, TiO₂/p-CdTe photovoltaic devices with efficiency of 1.8% were fabricated and their characteristic ‘enhancement’ is discussed.

© 2015 Elsevier Ltd. All rights reserved.

1. Introduction

The efficiency of photovoltaic devices can be improved using large band gap semiconductor windows known as hetero-contact layers. The interest in transparent conducting oxides (TCO) as top contacts in optoelectronic and photovoltaic applications has been increasing recently. Photovoltaic devices with single-crystal *p*-type CdTe and hetero-junctions using stable oxides, such as In₂O₃:Sn (ITO), ZnO, and SnO₂ have been investigated. First photovoltaic devices based on *p*-type CdTe single crystals with electron-beam evaporated ITO window layers (with $\eta = 10.5\%$) were developed by a Stanford group in 1977, with $U_{OC} = 810$ mV, $J_{SC} = 20$ mA/cm², and $FF = 65\%$ [1]. In 1987, cells fabricated by the reactive deposition of In₂O₃, on *p*-type CdTe single crystals reached $\eta = 13.4\%$, with $U_{OC} = 892$ mV, $J_{SC} = 20.1$ mA/cm², and $FF = 74.5\%$ [2]. In this device, the CdTe (111) face was etched in bromine methanol prior to loading into vacuum for In₂O₃ deposition. The CdTe crystal had a carrier concentration of 6×10^{15} /cm³. The open circuit voltage of this cell remains the highest ever reported for a CdTe device. N. Adeeb et al. [3] investigated the properties of ITO/CdTe solar cell fabricated by spraying an alcohol solution of indium chloride and tin chloride on *n*-type single crystal CdTe. The maximum sensitivity of the ITO/CdTe cells in the visible range reaches 0.42 A/W. The efficiency of the solar cells without antireflection coating at AM1 condition is 6.2%. Photovoltaic devices with *n*-ZnO layers on *p*-type CdTe single crystals showed poorer junction behavior, with efficiency smaller than 9% and $U_{OC} =$

540 mV [4]. In view of the success of the investigations of photovoltaic devices based on oxide/semiconductor structures using CdTe, Si, and InP as absorbers, as well as titanium dioxide can be good alternatives in such applications.

Titanium dioxide has high transparency for visible light, large value of the refractive index, controllable specific resistance, good adhesion and high chemical resistance. Also, TiO₂ is environment friendly. In the current work, we investigated the influence of annealing in vacuum and H₂ atmospheres on the structural and optical properties of the as-deposited TiO₂ and Nb:TiO₂ thin films. The titanium dioxide thin films were synthesized by reactive RF magnetron sputtering. Using ITO/CdTe, ZnO/CdTe as model systems, we fabricated the TiO₂/p-CdTe photovoltaic structures and report here on the application of the films in photovoltaic devices.

2. Experimental details

For sample preparation, a Ti target of 99.5% purity was used in the sputtering process. To obtain doped films, sintered pellets made of Nb₂O₅ powder (99.999% purity) were placed on the titanium target in the circular high-intensity sputter track region. The sputtering chamber was evacuated down to 1×10^{-5} mbar by a turbo molecular pump. The distance between the target and the substrate was kept constant at 3 cm. The magnetron discharge was done in a gas mixture of Ar and O₂ while the gas content was kept constant by introduction of 21 sccm Ar (99.99%) and 7 sccm O₂ (99.99%) via independent mass-flow controllers. The working total pressure was kept at 5×10^{-2} mbar. During depositions, the RF power was kept constant at 100 W. The substrate temperature was slightly higher than the room temperature (below 90 °C). The deposition time was 8 h in all experiments.

* Corresponding author. Tel.: +373 69953854.
E-mail address: tpotlog@gmail.com (T. Potlog).

Before deposition, the glass substrates were sequentially sonicated in acetone and ethanol, followed by rinsing with distilled water and drying. After deposition, the first set of undoped TiO₂ films were vacuum-annealed in the residual atmosphere at 420 °C for 30 min in the deposition chamber, under a pressure of 4.0×10^{-5} mbar, and in hydrogen atmosphere at a pressure of 2.0×10^{-3} mbar. A second set of Nb-doped TiO₂ films was annealed at 420 °C for 30 min in hydrogen atmosphere under the same pressure like the first set. We labeled the first set of TiO₂ samples as T₂ and the second set as TNb₂.

To evaluate the effects of TiO₂ films properties on solar cell characteristics, CdTe junction solar cells were subsequently fabricated. CdTe thin films were deposited by the close space sublimation method on the Nb:TiO₂-covered glass substrates annealed in H₂ atmosphere at 420 °C. The deposition of CdTe thin films was done at substrate temperature of $T_s = 320$ °C and evaporation temperature of $T_{ev} = 590$ °C. Further on, the CdTe layer was activated in chlorine atmosphere for 30 min at 400 °C. It has been demonstrated by various groups [5,6] that post-growth treatment with Cl is essential in promoting high performance in CdTe solar cells. According to the authors [7] the factor that identifies the p-doping of the CdTe thin films is the formation of the defect complexes such as $V_{Cd} + Cl_{Te}$. More than that, in the paper [8] we have investigated the chemical composition before and after CdCl₂ treatment and EDX analysis revealed that the ratio of at% of Cd and Te in as-deposited CdTe sample is 48.49:51.51. The lower Cd content gives rise to the formation of vacancies of Cd (V_{Cd}) in the CdTe lattice which act as acceptor centers. Also, CdTe films after CdCl₂ annealing contain an excess of Te. According to [7] the substitution of chlorine at the position of Te (Cl_{Te}) behave as a donor and annealing at 420 °C enriches material with Te vacancies and Cd whereas annealing of undoped CdTe increases the concentration of cadmium vacancies and increases the Te excess. Interaction between the V_{Cd} acceptor and Cl_{Te} causes the formation of the defect complexes such as $V_{Cd} + Cl_{Te}$ which improves the doping efficiency. Indium and nickel ohmic contacts for TiO₂ and p-CdTe thin films were deposited by thermal evaporation.

The structure of the films was investigated by X-ray diffraction (XRD) using a Bruker-AXS D8 Advance diffractometer (CuK_α radiation, 40 mA, 40 kV). The weight percentage of the anatase phase, W_A , was determined using the equation [9]:

$$W_A = \frac{1}{1 + 1.265^{I_R/I_A}},$$

where I_A and I_R are the intensities of the strongest anatase A(101) and rutile R(110) peaks, respectively. As discussed in the literature, the I_R/I_A ratio is independent of the fluctuations in diffractometer characteristics [9]. The grain size was calculated from the XRD patterns according to the Scherrer equation [10]:

$$D = \frac{0.9\lambda}{\beta \cos\theta},$$

where β is the diffraction half-height peak width for a Bragg angle θ , and λ is the wavelength of the X-ray radiation.

The surface morphology was investigated using an NT-MDT Solver Pro-M atomic force microscope operated in tapping mode. X-ray Photoelectron Spectroscopy measurements, using a Physical Electronics PHI 5000 VersaProbe instrument, were carried out to determine the surface elemental composition of the samples and the oxidation state of the elements. A double-beam Perkin-Elmer Lambda 19 UV-VIS spectrophotometer was used to record transmission spectra in the 300–1000 nm wavelength range.

The photovoltaic characteristics of solar cells were evaluated from the current–voltage characteristics, under 100 mW/cm² illumination, by means of a Spectra Physics Oriel 300 W Solar Simulator.

3. Results and discussion

3.1. Morphology, structure and oxidation states

The diffraction patterns of the first set of the as-deposited, the vacuum and the hydrogen-annealed samples are shown in Fig. 1A. The diffraction peaks were assigned to reflections corresponding to the anatase A(101) and rutile R(110) phases of TiO₂. For the as-deposited TiO₂ film, the weight percentage of the anatase phase (W_A) is 59.3% as calculated with Eq. (1). For vacuum-annealed film the weight percentage of the anatase phase (W_A) increases to 62%. The TiO₂ films annealed in H₂ atmosphere exhibits only the anatase phase. This increase in anatase concentration may result from a larger film thickness [11] and/or as an effect of doping (see Fig. 1A and B). The same effect, due to hydrogen annealing is significantly larger in the doped samples (see Fig. 1B (a) and (b)), compared to the undoped ones (Fig. 1B (a) and (b)). The effect of film thickness on material crystallinity will be further discussed in the next section.

The annealing in hydrogen of the pristine TiO₂ samples resulted in an increase in the average grain size from 51 nm to 88.4 nm and an enhancement of film crystallinity, as demonstrated by the increase of the intensity of the diffraction peak at $2\theta = 25.2^\circ$ in the XRD plots of the doped samples. Moreover, the peak position of the anatase A (101) peak shifts to a smaller diffracting angle (25.09°). No characteristic peaks of Nb₂O₅ were observed in Nb-doped TiO₂ thin films. This may

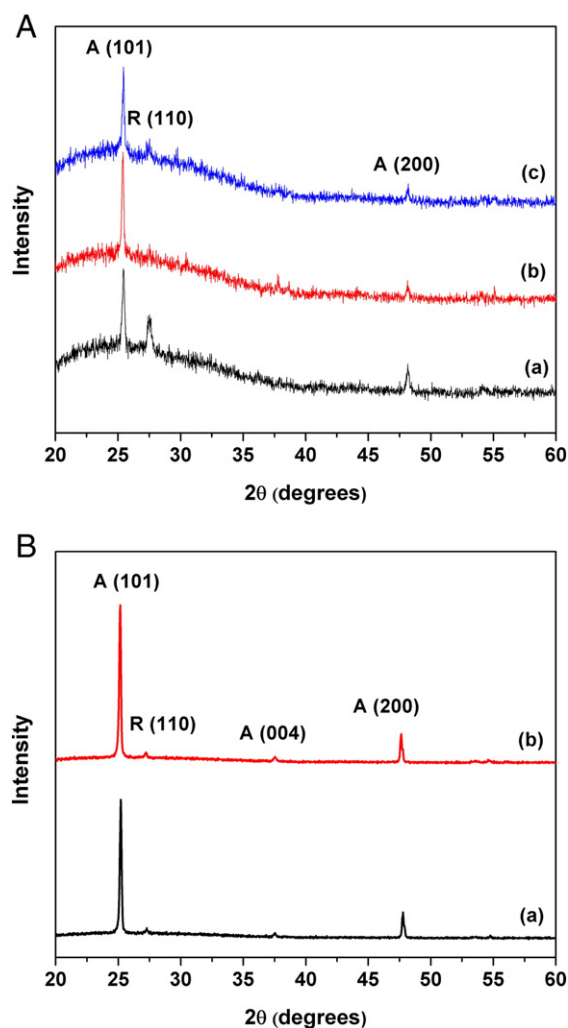


Fig. 1. A: The XRD patterns of: (a) as-deposited TiO₂ film; (b) H₂ annealed TiO₂ film; (c) vacuum-annealed TiO₂ film. B: The XRD patterns of: (a) Nb-doped TiO₂ film; (b) hydrogen annealed Nb-doped TiO₂ film.

Download English Version:

<https://daneshyari.com/en/article/828328>

Download Persian Version:

<https://daneshyari.com/article/828328>

[Daneshyari.com](https://daneshyari.com)